Halogen, hydrogen and electrostatic interactions in 2-amino-5-chloro-1,3-benzoxazol-3-ium nitrate and 2-amino-5-chloro-1,3-benzoxazol-3-ium perchlorate

Rafal Kruszynski* and Agata Trzesowska-Kruszynska

Institute of General and Ecological Chemistry, Technical University of Łódź, Zeromskiego 116, 90-924 Łódź, Poland
Correspondence e-mail: rafal.kruszynski@p.lodz.pl

In the title compounds, $C_7H_6ClN_2O^+ \cdot NO_3^-$ and $C_7H_6ClN_2O^+ \cdot ClO_4^-$, the ions are connected by $N—H \cdots O$ hydrogen bonds and halogen interactions. Additionally, in the first compound, co-operative $\pi–\pi$ stacking and halogen$\cdots\pi$ interactions are observed. The energies of the observed interactions range from a value typical for very weak interactions (1.80 kJ mol^{-1}) to one typical for mildly strong interactions (53.01 kJ mol^{-1}). The iminium cations exist in an equilibrium form intermediate between exo- and endocyclic. This study provides structural insights relevant to the biochemical activity of 2-amino-5-chloro-1,3-benzoxazole compounds.

Comment

Benzoxazole derivatives are important heterocyclic compounds that exhibit biological activities, including antitumour, antibacterial, DNA-damaging genotoxic and antiviral properties (Sum *et al.*, 2003; Oksuzoglu *et al.*, 2007; Tekiner-Gulbas *et al.*, 2007; Jauhari *et al.*, 2008). Recently, a novel series of benzoxazole derivatives have been developed as 5-HT3 receptor partial agonists for the treatment of diarrhoea-predominant irritable bowel syndrome (Yoshida *et al.*, 2005). Among them, the 2-substituted benzoxazole 2-amino-5-chloro-1,3-benzoxazole (2-abox) was found to be very active as a uricosuric and muscle relaxant, but the molecular and cellular mechanisms of action are not understood (McMillen *et al.*, 1992; Cao *et al.*, 2001; Liu *et al.*, 2003). Although its side effects limit its pharmaceutical usefulness, 2-abox has been used extensively in preclinical biological modelling studies, as a benchmark standard or as a model substrate for enzyme-catalysed oxidation (Wei *et al.*, 2000). Since the target binding site is unknown, studies of the bonding properties of 2-abox itself can be crucial for the design of new muscle-relaxant drugs.

In the Cambridge Structural Database (CSD, Version 5.30; Allen, 2002), five 2-abox adducts were found with organic compounds containing a carboxyl or carboxylate group (Lynch, Daly & Parsons, 2000; Lynch, Singh & Parsons, 2000; Lynch *et al.*, 2003), and two of these are proton-transfer salts. There are as yet no examples of the incorporation of this benzoxazole into salts with inorganic acids. As protonation is a common process occurring in physiological systems, and almost all drugs or bioactive molecules undergo protonation before they enter the reaction chain, knowledge of long-range interactions such as ion pairing might be helpful in the design of new drugs. In this context, the synthesis of 2-abox adducts with inorganic acids is of interest. Hence, the solid-state characterization of 2-amino-5-chloro-1,3-benzoxazol-3-ium nitrate, (I), and 2-amino-5-chloro-1,3-benzoxazol-3-ium perchlorate, (II), as well as the results of quantum mechanical calculations, are reported here.
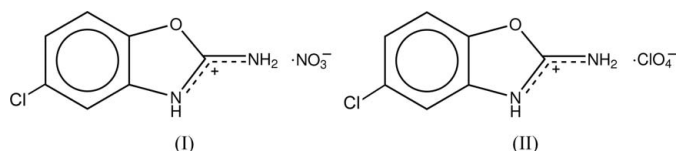
The asymmetric units of (I) and (II) contain an inorganic anion acting as counter-ion, balancing the charge of the 2-abox cation (Figs. 1 and 2). The 2-abox cation is close to being planar, with maximum deviations from the weighted least-squares plane calculated for its all non-H atoms of 0.0434 (15) and 0.0119 (12) Å for atoms N2, for (I) and (II), respectively. The weighted least-squares plane defined by the atoms of the nitrate group in (I), with a maximum deviation of 0.0063 (15) Å for atom N3, is inclined at 10.30 (10)° to the plane of the cation. The bond lengths and angles (Tables 1 and 2) in the 2-abox cations of (I) and (II) are consistent with those in pure 2-abox (Lynch, 2004), except for the C—N and C—O distances. The C1—N2 and C1—O1 bonds are shortened [by 0.040 (3) and 0.035 (2) Å, respectively, for (I), and by 0.039 (3) and 0.035 (2) Å, respectively, for (II)], while the C1—N1 bonds are elongated by 0.021 (3) and 0.018 (3) Å, respectively, for (I) and (II), compared with neutral 2-abox. Similar effects can be observed for 2-abox adducts or salts with organic compounds (Lynch, Daly, & Parsons, 2000; Lynch, Singh & Parsons, 2000; Lynch *et al.*, 2003). This lengthening (compared with neutral 2-abox) observed in (I) and (II) is caused by protonation of the endocyclic N atom of the five-membered heterocyclic ring, together with the strong hydrogen-bond acceptor properties of the O atoms of the anion involved in intermolecular $N_{endocyclic}—H \cdots O$ hydrogen bonds. In 2-abox, this endocyclic N atom acts as a hydrogen-bond acceptor in intermolecular $N—H \cdots N$ hydrogen bonds. For similar 2-aminoheterocyclic compounds, shortening of the exocyclic C—N bond (compared with neutral 2-abox) has been explained by the attraction of a more electron-accepting heterocyclic ring (Lynch & Jones, 2004). This suggests the delocalization of electron density and in consequence delocalization of the positive charge over the $HN—C—NH_2$ moiety. Such exocyclic imines or iminium ions in equilibrium

organic compounds
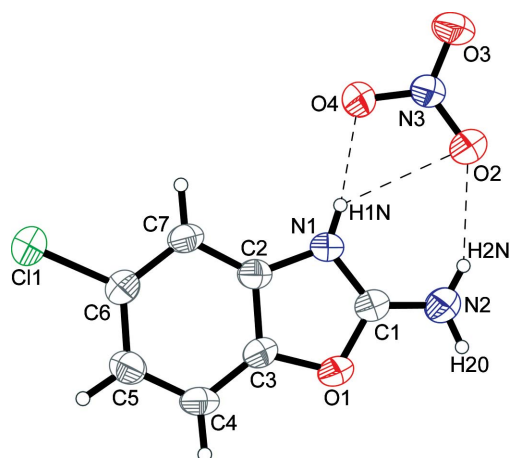
Figure 1
A view of the asymmetric unit of (I), showing the atom-labelling scheme. Displacement ellipsoids are drawn at the 50% probability level and H atoms are shown as spheres of arbitrary radii. Hydrogen bonds are indicated by dashed lines.
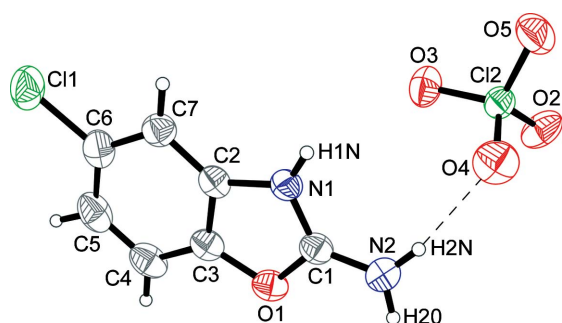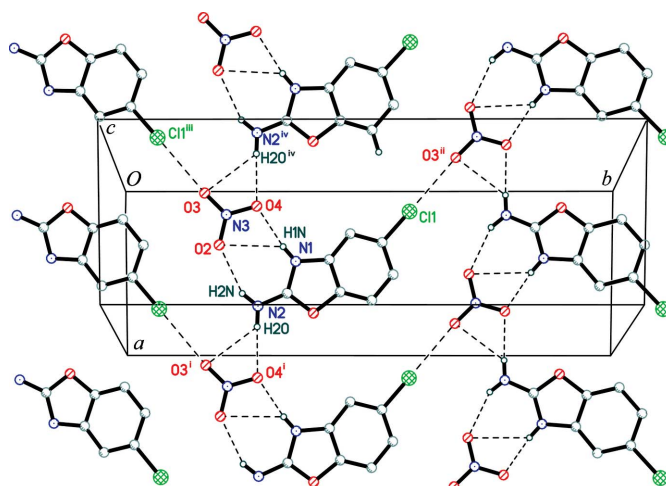

Figure 2
A view of the asymmetric unit of (II), showing the atom-labelling scheme. Displacement ellipsoids are drawn at the 50% probability level and H atoms are shown as spheres of arbitrary radii. The dashed line indicates a hydrogen bond.

Figure 3
Part of the molecular packing of (I), showing the N—H···O hydrogen bonds and Cl···O halogen interactions (dashed lines). H atoms not involved in intermolecular interactions have been omitted for clarity. [Symmetry codes: (i) $x + 1, y, z$; (ii) $-x, y + \frac{1}{2}, -z + \frac{1}{2}$; (iii) $-x, y - \frac{1}{2}, -z + \frac{1}{2}$; (iv) $x - 1, y, z$.]

Figure 4
Part of the molecular packing of (II), showing the N—H···O hydrogen bonds as dashed lines. H atoms not involved in intermolecular interactions have been omitted for clarity. [Symmetry codes: (i) x, $-y + \frac{1}{2}, z - \frac{1}{2}$; (ii) $x - 1, y, z$.]
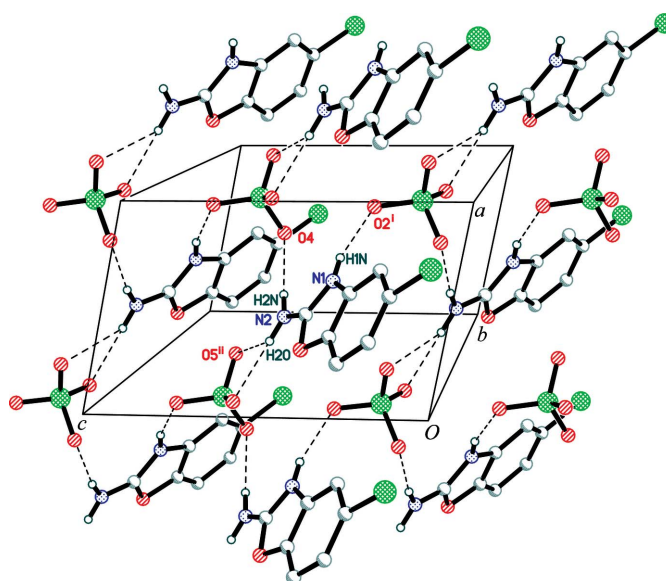
with endocyclic imines or iminium ions have been found previously and discussed for other compounds containing the $N_{exo}CN_{endo}$ group (Lynch & Jones, 2004; Low *et al.*, 2003; Donga *et al.*, 2002; Trzesowska-Kruszynska & Kruszynski, 2009; Kruszynski & Trzesowska-Kruszynska, 2009).

The ions in (I) and (II) are linked by hydrogen bonds, $\pi-\pi$ stacking and halogen interactions. The crystal structure of (I) is stabilized by amine–nitrate N—H···O hydrogen bonds (Table 3), which form an $N_2 = R_1^2(4)R_2^2(4)R_2^1(6)[C_2^1(6)C_2^2(6)-C_2^2(6)]$ basic graph set (Bernstein *et al.*, 1995), and in consequence form hydrogen-bonded chains along the [100] axis (Fig. 3). Noteworthy is the fact that one second-level $R_1^2(4)$ and one second-level $R_2^1(6)$ basic motif create a binary $R_2^2(8)$ complex graph. The benzene rings and nitrate anions of successive hydrogen-bonded chains are interlinked by C—H···O interactions, so forming a folded two-dimensional net parallel to (001).

As in (I), so in (II) the N—H···O hydrogen bonds create finite D motifs in terms of unitary level graphs, but on the second level the motifs are more complicated and can be expressed by an $N_2 = R_1^2(4)R_2^2(8)D[C_1^2(4)C_2^2(6)D][R_1^2(4)C_2^2(8)-D]$ descriptor of basic graph set or, more simply, as an $N_2 = C_1^2(4)C_2^3(12)$ complex graph set. The N—H···O hydrogen bonds expand the ions of (II) into a folded two-dimensional net along the (010) plane (Fig. 4). Thus, the change from a planar nitrate group to a tetrahedral perchlorate group leads to an elaboration of the N—H···O hydrogen-bonded chain in (I) to the hydrogen-bonded net of (II), accompanied by more complex graph-set motifs.

In (I), $\pi-\pi$ stacking interactions (Hunter & Sanders, 1990) can be observed (Table 3) between benzene rings, parallel by symmetry, of adjacent 2-amino-5-chlorobenzoxazolium ions oriented in opposite directions (Fig. 5). In this way, a $\pi-\pi$ stacked pile along the [001] axis is created. In one of the above-mentioned arrangements of interacting cations [that in

which the cations are related by an inversion centre at $(\frac{1}{2}, \frac{1}{2}, \frac{1}{2})$], the Cl atom is situated almost above the oxazolium ring centroid (Fig. 5) at a distance of 3.411 (3) Å, with an angle between the vector linking the ring centroid and atom Cl1 of 86.07 (2)° and a distance between the oxazolium ring plane and atom Cl1 of 3.403 Å. This contact can be considered a bonding interaction, since the Cl$\cdots\pi$ distance fulfils the criterion (Schottel *et al.*, 2008; Imai *et al.*, 2008) of being shorter than the sum of the Cl and C van der Waals radii (3.45 Å; Bondi, 1964). This suggests that π–π stacking inter- actions have a synergistic effect on forming halogen$\cdots\pi$ interactions. Usually, the existence of other co-operative interactions is required to create a weaker halogen$\cdots\pi$ contact (Escudero *et al.*, 2009; Imai *et al.*, 2008). There are short contacts between the cations of (II), but the possibility of π–π interactions was rejected on geometric grounds (neigh- bouring aromatic/delocalized bonds do not overlap suffi- ciently). Despite the fact that the Cl atom in (II) is situated almost above the benzene ring centroid, the possibility of a Cl$\cdots\pi$ contact was rejected on the basis of too long a Cl$\cdots\pi$ distance, larger than the sum of the Cl and C van der Waals radii.

An interesting feature of the structures of (I) and (II) is the presence of halogen interactions. In (I), there is a short intermolecular C6—Cl1$\cdots$O3^{viii}═N3^{viii} contact [Fig. 3; symmetry code: (viii) $-x, y + \frac{1}{2}, -z + \frac{1}{2}$] of 2.989 (2) Å, shorter than the sum of the van der Waals radii (3.27 Å; Bondi, 1964), with a C6—Cl1$\cdots$O3^{viii} angle of 176.1 (2)°. In (II), the similar C6—Cl1$\cdots$O5^{ix}═Cl2^{ix} contact [symmetry code: (ix) $-x + 2, y - \frac{1}{2}, -z + \frac{1}{2}$] is slightly longer [3.152 (2) Å] and the C6— Cl1$\cdots$O5^{ix} angle is smaller [165.2 (2)°].

A search of the CSD yielded nine compounds containing the chlorophenyl moiety in close contact with the O atom of the nitrate ion. The average intermolecular Cl$\cdots$O distance from 11 hits is 3.16 (7) Å, slightly longer than that observed in (I). An analogous search carried out for a chlorophenyl moiety and a perchlorate ion gives 40 compounds, with 44 interactions and a mean distance of 3.14 (2) Å, which is the same as that in (II), within experimental error. In the other known 2-abox adducts or salts with organic compounds (Lynch, Daly & Parsons, 2000; Lynch, Singh & Parsons, 2000; Lynch *et al.*, 2003), the Cl atom is either involved in hydrogen bonding or forms Cl$\cdots$Cl contacts, but Cl$\cdots$O contacts were not observed.

The CSD was also searched for all intermolecular C— Cl$\cdots$O(N) and C—Cl$\cdots$O(Cl) contacts shorter than 3.27 Å (sum of the van der Waals radii; Bondi, 1964). The most common acceptor of halogen bonds is the O atom of the nitrate or perchlorate group, respectively. The number of reported Cl$\cdots$O interactions decreases rapidly as the Cl$\cdots$O distance shortens below 3.0 Å. Less than 5% of Cl$\cdots$O interactions can be considered as relatively strong. The C— Cl$\cdots$O and Cl$\cdots$O(N/Cl) angles adopt values in the range 70– 180°, with a single maximum of 165° for the C—Cl$\cdots$O angle and multiple maxima in the range 100–170° for the Cl$\cdots$O(N/ Cl) angles. Examination of two-dimensional contour plots of angles *versus* distances reveals between one and four
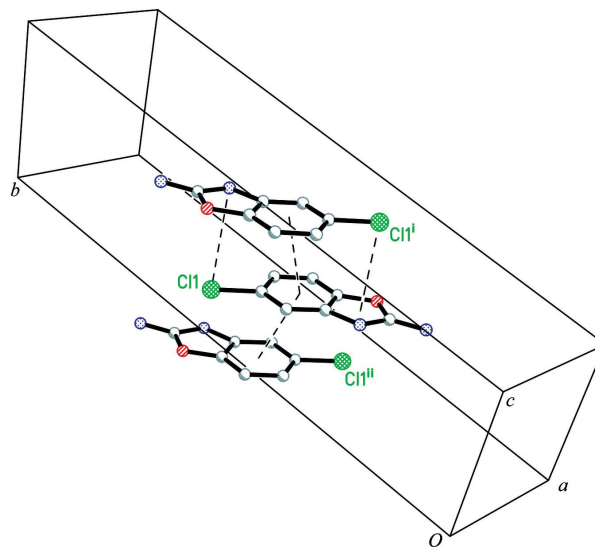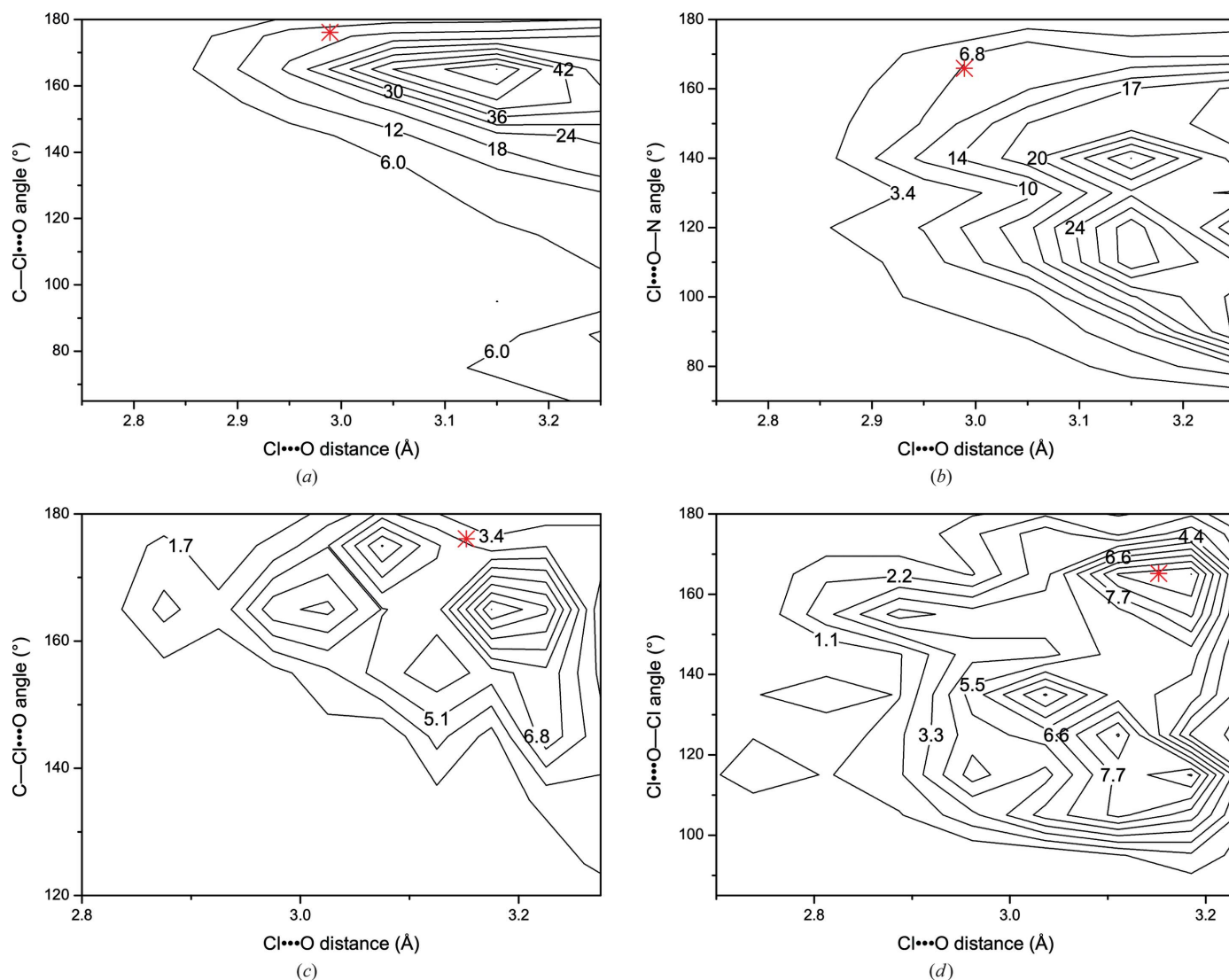

Figure 5
Part of the molecular packing of (I), showing the Cl$\cdots\pi$ and π–π stacking interactions (dashed lines) between 2-abox cations. H atoms have been omitted for clarity. [Symmetry codes: (i) $-x + 1, -y + 1, -z + 1$; (ii) $-x + 1, -y + 1, -z$.]

preferred distance–angle pairs (Fig. 6), with the most popu- lated maxima at 3.143 Å and 163.5°, 3.152 Å and 139.4°, 3.177 Å and 165.6°, and 3.174 Å and 163.4° for Cl$\cdots$O distances and C—Cl$\cdots$O$_N$, Cl$\cdots$O(N), C—Cl$\cdots$O$_{Cl}$ and Cl$\cdots$O(Cl) angles, respectively. The distances in (I) and (II) are shorter and the angles are larger than the most preferred ones.

The molecular electronic properties have been calculated for (I) and (II) at a single point for both the diffraction- derived coordinates and the optimized structures, and these are comparable within three standard deviations, although the geometrically optimized molecules show typical elongation of the C—H bonds (0.15–0.21 Å). The total binding energies of the intermolecular interactions were calculated for molecular sets containing from one to four cation–anion pairs. The cation and anion of each pair were arranged as in the hydrogen- bonded sheets, along the halogen bonds and in the π–π stacking interactions. In order to estimate the energy of the electrostatic interactions between the anions and cations, additional computations were performed for subsets containing an odd number of cations and anions. Basis-set superposition error (BSSE) corrections were carried out using the counterpoise (CP) method (Boys & Bernardi,1970). The B3LYP functional (Becke, 1993; Lee *et al.*, 1988) in the triple-ζ 6-311++G(3df,2p) basis set was used, as implemented in *GAUSSIAN03* (Frisch *et al.*, 2004). In all cases, the differences in electronic properties and energies originating from the different numbers of cation–anion pairs used in the calcula- tion, and the differences between the various methods described above, are given in parentheses as standard uncer- tainties of the mean values. Where a deviation is not given, the values were the same within their range of reported precision.

As expected, the cations and anions of (I) and (II) are attracted by strong electrostatic interactions with very large binding energies of 337.23 and 344.34 kJ mol^{-1}, respectively.

Figure 6
Contour plots, showing the relationship between the C—Cl···O or Cl···O(N/Cl) angles and the Cl···O distances for (a)/(b) (I) and (c)/(d) (II). The values for (I) or (II) are indicated by asterisks and the contours are frequency of occurrence.

The energy of the π–π stacking interaction between the 2-abox cations of (I) related by the inversion centre at $(\frac{1}{2}, \frac{1}{2}, 0)$, as calculated by the total self-consistent field-energy method, proves that this interaction has antibonding character (excluding the dispersion energy). The co-operative effect of the π–π stacking and halogen···π interactions between 2-abox cations related by the symmetry operator $(-x + 1, -y + 1, -z + 1)$ is manifested by the larger value of the total binding energy, which is 3.56 (4) kJ mol^{-1}. The energies of the Cl···O intermolecular interactions are 15.48 (8) and 6.28 (4) kJ mol^{-1}, respectively, for (I) and (II), which is in accordance with the energies of intermolecular halogen bonds present in small molecules (Allen *et al.*, 1997; Zou *et al.*, 2005; Kruszynski, 2007).

Previously, it was postulated that an electric attraction exists between the N—Cl and O=C groups of *N*-chlorosuccinimide, due to polarization of these groups (Brown, 1961), N$^{\delta-}$—Cl$^{\delta+}$···O$^{\delta-}$=C$^{\delta+}$, and such a model of polarization was confirmed for 1,3-dibromo-5,5-dimethylimidazolidine-2,4-di-

one (Kruszynski, 2007). Analysis of the atomic charges based on the Breneman radii (Breneman & Wiberg, 1990) shows that similar polarization also exists for (I) and (II). The C-bonded Cl atoms have a partial charge of 0.011 (5) a.u. for both studied compounds, and the aromatic ring C atoms are negatively charged. The anion O atoms have mean charges of -0.72 and -0.60 a.u., respectively, for NO$_3^-$ and ClO$_4^-$, and the N and Cl atoms of the anions have charges of 1.20 (3) and 1.41 (1) a.u., respectively. The positive charge located on the Cl atom is relatively small but, combined with the large negative charge present on the O atoms of the anions, Cl···O interactions are electrostatically permitted.

The results of the quantum-mechanical calculations indicate that stronger hydrogen bonds are more attractive than halogen bonds. The values of the hydrogen-bond energies lie in ranges typical for similar hydrogen bonds (Desiraju & Steiner, 1999). The total energy of three N—H···O hydrogen bonds formed between a 2-abox cation and a nitrate ion (Fig. 1 and Table 2) is 56.10 (8) kJ mol^{-1}, whereas the total energy of

those formed between a cation and anion related by the symmetry operator ($x + 1$, y, z) is 41.84 (8) kJ mol^{-1}. As expected, the C—H···O hydrogen-bond energy is small (Table 3) and comparable with those for small-angle N—H···O hydrogen bonds. In general, bonds with very similar geometry are stronger in (II) than in (I), suggesting that the topology of the electron-density distribution in the anion significantly influences the strength of the hydrogen bonds.

The noncovalent nature of the intermolecular interactions in (I) and (II) was analysed using the natural bond orbital (NBO) method (Foster & Weinhold, 1980; Reed & Weinhold, 1985; Reed *et al.*, 1988). In this method, the strength of the donor–acceptor charge-transfer delocalization is characterized by the second-order stabilization energy, E_{del}. For halogen bonds, the principal charge-transfer interactions occur between the O-atom lone pairs and the antibonding orbitals of the C—Cl bond [E_{del} = 12.89 (3) and 5.69 kJ mol^{-1}, respectively, for (I) and(II)], and lateral charge-transfer interactions occur between the O-atom lone pairs and the one-centre Rydberg orbitals of the Cl atom. A similar scheme is observed for the hydrogen bonds: the hydrogen-bond acceptor lone pairs donate their lone-pair electron density primarily to the antibonding orbitals of the hydrogen-bond donor and secondarily to the Rydberg orbitals of the H atom. The origins of the observed stacking (based on NBO calculations) are the interactions of the delocalized molecular π orbitals of one molecule with the delocalized antibonding molecular π orbitals and antibonding molecular σ orbital created between the C atoms of the second aromatic ring, and *vice versa*. The interactions with the antibonding molecular σ orbitals contribute a larger proportion (about 70%) of the total intermolecular binding energy than those with the delocalized antibonding molecular π orbitals. This confirms the generally accepted model of stacking interactions, which postulates that the interactions appear when attractive interactions between π electrons and the σ framework outweigh unfavourable contributions such as π-electron repulsion (Hunter & Sanders, 1990).

Experimental

A hot ethanolic solution (4 ml) of 2-amino-5-chloro-1,3-benzoxazole (0.150 g, 1 mmol) was mixed with either 65% nitric acid (5 ml) [for the preparation of (I)] or 60% perchloric acid (5 ml) [for the preparation of (II)]. The resulting solutions were allowed to cool to room temperature and, after several days, orange crystals of (I) and dark-red crystals of (II) suitable for X-ray diffraction were isolated in yields of 69 and 78%, respectively.

Compound (I)

Crystal data

$C_7H_6ClN_2O^+\cdot NO_3^-$	V = 933.9 (2) Å^3
M_r = 231.60	Z = 4
Monoclinic, $P2_1/c$	Mo $K\alpha$ radiation
a = 6.8900 (9) Å	μ = 0.41 mm^{-1}
b = 20.3139 (18) Å	T = 291 K
c = 7.2562 (10) Å	$0.11 \times 0.09 \times 0.08$ mm
β = 113.138 (9)°	

Table 1
Selected bond lengths (Å) for (I).

N1—C1	1.325 (2)	O1—C3	1.400 (2)
N1—C2	1.392 (2)	N3—O3	1.216 (2)
C1—N2	1.294 (3)	N3—O2	1.238 (2)
C1—O1	1.339 (2)	N3—O4	1.251 (2)

Table 2
Selected bond lengths (Å) for (II).

N1—C1	1.322 (2)	Cl2—O5	1.4236 (14)
N1—C2	1.400 (2)	Cl2—O4	1.4359 (14)
C1—N2	1.295 (2)	Cl2—O3	1.4361 (13)
C1—O1	1.339 (2)	Cl2—O2	1.4366 (13)
O1—C3	1.401 (2)		

Data collection

Kuma KM-4 CCD area-detector diffractometer	12495 measured reflections
Absorption correction: numerical (*X-RED*; Stoe & Cie, 1999)	1642 independent reflections
T_{min} = 0.955, T_{max} = 0.968	1593 reflections with $I > 2\sigma(I)$
	R_{int} = 0.017

Refinement

$R[F^2 > 2\sigma(F^2)]$ = 0.035	136 parameters
$wR(F^2)$ = 0.091	H-atom parameters constrained
S = 1.17	$\Delta\rho_{max}$ = 0.26 e Å^{-3}
1642 reflections	$\Delta\rho_{min}$ = −0.18 e Å^{-3}

Compound (II)

Crystal data

$C_7H_6ClN_2O^+\cdot ClO_4^-$	V = 1039.7 (2) Å^3
M_r = 269.04	Z = 4
Monoclinic, $P2_1/c$	Mo $K\alpha$ radiation
a = 6.1743 (8) Å	μ = 0.63 mm^{-1}
b = 17.6159 (19) Å	T = 291 K
c = 9.7682 (11) Å	$0.19 \times 0.19 \times 0.16$ mm
β = 101.869 (9)°	

Data collection

Kuma KM-4 CCD area-detector diffractometer	14071 measured reflections
Absorption correction: numerical (*X-RED*; Stoe & Cie, 1999)	1829 independent reflections
T_{min} = 0.888, T_{max} = 0.896	1774 reflections with $I > 2\sigma(I)$
	R_{int} = 0.015

Refinement

$R[F^2 > 2\sigma(F^2)]$ = 0.027	145 parameters
$wR(F^2)$ = 0.071	H-atom parameters constrained
S = 1.06	$\Delta\rho_{max}$ = 0.21 e Å^{-3}
1829 reflections	$\Delta\rho_{min}$ = −0.28 e Å^{-3}

H atoms bonded to C atoms were treated as riding atoms in calculated positions, with C—H = 0.93 Å and U_{iso}(H) = 1.2U_{eq}(C). H atoms bonded to N atoms were located in difference maps and then permitted to ride at the positions deduced from the difference maps, with U_{iso}(H) = 1.2U_{eq}(N), giving the N—H distances shown in Table 3.

For both compounds, data collection: *CrysAlis CCD* (UNIL IC & Kuma, 2000); cell refinement: *CrysAlis RED* (UNIL IC & Kuma, 2000); data reduction: *CrysAlis RED*; program(s) used to solve structure: *SHELXS97* (Sheldrick, 2008); program(s) used to refine structure: *SHELXL97* (Sheldrick, 2008); molecular graphics: *XP* in

Table 3
Experimental hydrogen-bond geometry (Å, °) for (I) and (II), total energy E (kJ mol^{-1}) and principal 'delocalization' energy E_{del}, calculated on the natural bonding orbital basis.

θ is the $D-H\cdots A$ angle.

$D-H\cdots A$	$D-H$	$H\cdots A$	$D\cdots A$	θ	E	E_{del}
(I)						
N1—H1N$\cdots$O4	0.78	1.96	2.735 (2)	172	39.85 (5)	27.246 (8)
N1—H1N$\cdots$O2	0.78	2.57	3.152 (2)	132	3.640 (12)	3.326 (1)
N2—H2N$\cdots$O2	0.80	2.14	2.886 (2)	154	12.62 (4)	8.857 (3)
N2—H2O$\cdots$O4^i	0.83	2.08	2.908 (2)	172	39.36 (6)	24.233 (4)
N2—H2O$\cdots$O2^i	0.83	2.58	3.171 (3)	129	2.48 (4)	2.192
C5—H5$\cdots$O2^{ii}	0.93	2.49	3.386 (3)	162	3.14 (8)	2.410 (1)
(II)						
N1—H1N$\cdots$O2^{iii}	0.82	2.05	2.8527 (19)	166	42.29 (2)	25.878 (8)
N2—H2N$\cdots$O4	0.85	2.10	2.932 (2)	168	53.01 (8)	34.116 (11)
N2—H2O$\cdots$O3^{iv}	0.86	2.13	2.989 (2)	177	38.38 (7)	25.057 (9)
N2—H2O$\cdots$O5^{iv}	0.86	2.55	3.103 (2)	123	2.04 (7)	1.786
C4—H4$\cdots$O3^v	0.93	2.59	3.289 (2)	132	10.29 (8)	8.372

Symmetry codes: (i) $x + 1, y, z$; (ii) $-x + 1, y + \frac{1}{2}, -z + \frac{1}{2}$; (iii) $x, -y + \frac{1}{2}, z - \frac{1}{2}$; (iv) $x - 1, y, z$; (v) $-x + 1, -y, -z + 1$.

SHELXTL/PC (Sheldrick, 2008) and *ORTEP-3 for Windows* (Version 1.062; Farrugia 1997); software used to prepare material for publication: *SHELXL97* and *PLATON* (Spek, 2009).

Table 4
Experimental geometry of stacking interactions (Å, °) for (I).

$Cg6$ is the ring centroid of the six-membered ring. $Cg\cdots Cg$ is the perpendicular distance between the first ring centroid and that of the second ring. α is the dihedral angle between planes J and K. β is the angle between the vector linking the ring centroids and the normal to ring J. CgJ_{perp} is the perpendicular distance from the J ring centroid to ring K.

$CgJ\cdots CgK$	$Cg\cdots Cg$	α	β	CgJ_{perp}
$Cg6\cdots Cg6^{vi}$	3.745 (3)	0	25.3 (2)	3.385 (3)
$Cg6\cdots Cg6^{vii}$	3.737 (3)	0	26.1 (2)	3.355 (3)

Symmetry codes: (vi) $-x + 1, -y + 1, -z$; (vii) $-x + 1, -y + 1, -z + 1$.

References

Allen, F. H. (2002). *Acta Cryst.* B**58**, 380–388.
Allen, F. H., Lommerse, J. P. M., Hoy, V. J., Howard, J. A. K. & Desiraju, G. R. (1997). *Acta Cryst.* B**53**, 1006–1016.
Becke, A. D. (1993). *J. Chem. Phys.* **98**, 5648–5652.
Bernstein, J., Davis, R. E., Shimoni, L. & Chang, N.-L. (1995). *Angew. Chem. Int. Ed. Engl.* **34**, 1555–1573.
Bondi, A. (1964). *J. Phys. Chem.* **68**, 441–451.
Boys, S. F. & Bernardi, F. (1970). *Mol. Phys.* **19**, 553–566.
Breneman, C. M. & Wiberg, K. B. (1990). *J. Comput. Chem.* **11**, 361–373.
Brown, R. N. (1961). *Acta Cryst.* **14**, 711–715.
Cao, Y.-J., Dreixler, J. C., Roizen, J. D., Roberts, M. T. & Houamed, K. M. (2001). *J. Pharmacol. Exp. Ther.* **296**, 683–689.
Desiraju, G. R. & Steiner, T. (1999). *The Weak Hydrogen Bond in Structural Chemistry and Biology.* New York: Oxford University Press Inc.
Donga, H.-S., Quan, B. & Tian, H.-Q. (2002). *J. Mol. Struct.* **641**, 147–152.
Escudero, D., Frontera, A., Quinonero, D. & Deya, P. M. (2009). *J. Comput. Chem.* **30**, 75–82.
Farrugia, L. J. (1997). *J. Appl. Cryst.* **30**, 565.
Foster, J. P. & Weinhold, F. A. (1980). *J. Am. Chem. Soc.* **102**, 7211–7218.
Frisch, M. J., *et al.* (2004). *GAUSSIAN03.* Revision E.01. Gaussian Inc., Wallingford, Connecticut, USA.
Hunter, C. A. & Sanders, J. K. M. (1990). *J. Am. Chem. Soc.* **112**, 5525–5534.
Imai, Y. N., Inoue, Y., Nakanishi, I. & Kitaura, K. (2008). *Protein Sci.* **17**, 1129–1137.
Jauhari, P. K., Bhavani, A., Varalwar, S., Singhal, K. & Raj, P. (2008). *Med. Chem. Res.* **17**, 412–424.
Kruszynski, R. (2007). *Acta Cryst.* C**63**, o389–o391.
Kruszynski, R. & Trzesowska-Kruszynska, A. (2009). *Acta Cryst.* C**65**, o624–o629.
Lee, C., Yang, W. & Parr, R. G. (1988). *Phys. Rev. B*, **37**, 785–789.
Liu, Y.-C., Lo, Y.-K. & Wu, S.-N. (2003). *Brain Res.* **959**, 86–97.
Low, J. N., Cobo, J., Abonia, R., Insuasty, B. & Glidewell, C. (2003). *Acta Cryst.* C**59**, o669–o671.
Lynch, D. E. (2004). *Acta Cryst.* E**60**, o1715–o1716.
Lynch, D. E., Barfield, J., Frost, J., Antrobus, R. & Simmons, J. (2003). *Cryst. Eng.* **6**, 109–122.
Lynch, D. E., Daly, D. & Parsons, S. (2000). *Acta Cryst.* C**56**, 1478–1479.
Lynch, D. E. & Jones, G. D. (2004). *Acta Cryst.* B**60**, 748–754.
Lynch, D. E., Singh, M. & Parsons, S. (2000). *Cryst. Eng.* **3**, 71–79.
McMillen, B. A., Williams, H. L., Lehmann, H. & Shepard, P. D. (1992). *J. Neural Transm.* **89**, 11–25.
Oksuzoglu, E., Temiz-Arpaci, O., Tekiner-Gulbas, B., Eroglu, H., Sen, G., Alper, S., Yildiz, I., Diril, N., Aki-Sener, E. & Yalcin, I. (2007). *Med. Chem. Res.* **16**, 1–14.
Reed, A. E., Curtis, L. A. & Weinhold, F. A. (1988). *Chem. Rev.* **88**, 899–926.
Reed, A. E. & Weinhold, F. A. (1985). *J. Chem. Phys.* **83**, 1736–1740.
Schottel, B. L., Chifotides, H. T. & Dunbar, K. R. (2008). *Chem. Soc. Rev.* **37**, 68–83.
Sheldrick, G. M. (2008). *Acta Cryst.* A**64**, 112–122.
Spek, A. L. (2009). *Acta Cryst.* D**65**, 148–155.
Stoe & Cie (1999). *X-RED.* Version 1.18. Stoe & Cie GmbH, Darmstadt, Germany.
Sum, P.-E., How, D., Torres, N., Newman, H., Petersen, P. J. & Mansour, T. S. (2003). *Bioorg. Med. Chem. Lett.* **13**, 2607–2610.
Tekiner-Gulbas, B., Temiz-Arpaci, O., Yildiz, I. & Altanlar, N. (2007). *Eur. J. Med. Chem.* **42**, 1293–1299.
Trzesowska-Kruszynska, A. & Kruszynski, R. (2009). *Acta Cryst.* C**65**, o19–o23.
UNIL IC & Kuma (2000). *CrysAlis CCD* and *CrysAlis RED.* Versions 1.163. Kuma Diffraction Instruments GmbH, Wrocław, Poland.
Wei, P., Zhang, J., Egan-Hafley, M., Liang, S. & Moore, D. D. (2000). *Nature (London)*, **407**, 920–923.
Yoshida, S., Shiokawa, S., Kawano, K., Ito, T., Murakami, H., Suzuki, H. & Sato, Y. (2005). *J. Med. Chem.* **48**, 7075–7079.
Zou, J.-W., Jiang, Y.-J., Guo, M., Hu, G.-X., Zhang, B., Liu, H.-C. & Yu, Q.-S. (2005). *Chem. Eur. J.* **11**, 740–751.